Isotopic effect in the lattice parameter of rare-gas solids

2003 J. Phys.: Condens. Matter 15 475

(http://iopscience.iop.org/0953-8984/15/3/312)

INSTITUTE OF PHYSICS PUBLISHING JOURNAL OF PHYSICS: CONDENSED MATTER

J. Phys.: Condens. Matter **15** (2003) 475–488 PII: S0953-8984(03)54640-9

Isotopic effect in the lattice parameter of rare-gas solids

Carlos P Herrero

Instituto de Ciencia de Materiales, Consejo Superior de Investigaciones Científicas (CSIC), Campus de Cantoblanco, 28049 Madrid, Spain

Received 10 October 2002
Published 13 January 2003
Online at stacks.iop.org/JPhysCM/15/475

Abstract

The dependence of the lattice parameter of rare-gas (Lennard-Jones) solids on isotopic mass has been studied by the path-integral Monte Carlo method. Simulations were carried out in the isothermal–isobaric ensemble, which allows us to study this isotopic effect as a function of temperature and pressure. In the limit $T \to 0$ and at ambient pressure, the difference Δa between lattice parameters of isotopically pure crystals with lightest and heaviest isotopic mass is found to range from 8.7×10^{-3} Å for Ne to 1.2×10^{-3} Å for Xe. This isotopic effect decreases appreciably upon increasing temperature. At 80 K, Δa for Ar, Kr and Xe is found to be less than one-third of the corresponding low-temperature value. An applied hydrostatic pressure also causes an important decrease in Δa. For Ne and Xe, a pressure of 30 kbar reduces this difference by a factor of 6.5 and 3.1, respectively. These differences in lattice parameter are larger than the sensitivity limit presently achieved in experimental studies, even for solid xenon at its Debye temperature.

1. Introduction

The study of isotopic substitution occupies an old and important place in solid state research. Different types of isotopic effects have been studied over the years, some of which are due to the variation of phonon frequencies with the average isotopic mass [1]. This mass dependence of the frequencies causes changes in the average vibrational amplitudes. While at high temperatures these amplitudes are independent of the isotopic mass, at low temperatures they decrease with increasing mass, as a consequence of zero-point quantum motion, which manifests itself through the anharmonicity of the interatomic forces. The simplest anharmonic effect of this type is the dependence of the lattice parameters on isotopic masses, a quantum effect observable at a macroscopic scale: lighter isotopes produce larger lattice parameters. At temperatures higher than the Debye temperature of the solid considered, Θ_D, the isotope effect on the crystal volume becomes irrelevant and disappears in the high-temperature (classical) limit. Something similar happens for other crystal properties, such as compressibility or

heat capacity, which show maximum isotopic effects at low temperatures. Isotope effects on the unit-cell parameters have been studied in different kinds of crystals by experimental and theoretical techniques. In recent years, the isotope effect on the unit-cell parameters of crystalline materials has been measured with unprecedented precision by using x-ray standing waves [2, 3].

Rare-gas van der Waals solids form an important class of materials, which provide ideal systems allowing fruitful comparisons between theory and experiment. The simplicity of these solids makes them particularly interesting for studying structural and electronic transitions in detail. The interatomic forces are weak, short range and rather well understood, so that critical tests of appropriate theories by their ability to predict properties of rare-gas crystals are relatively simple. At ambient pressure these solids are transparent and nonconducting, and consist of spherically symmetric atoms crystallized into a face-centred cubic lattice. These properties make noble-gas crystals more amenable to theoretical treatment than many other solids. In particular, the thermodynamic properties of these weakly bound solids are interesting due to the large anharmonic contributions to their lattice dynamics. Solid helium is an extreme case where short-range correlation effects are very important. For heavier elements, quantum effects are less important, but some of them can still be observable at low temperatures, even for solid xenon, because of the large anharmonicity of the lattice vibrations.

Anharmonic effects in rare-gas solids have been studied theoretically by means of different approaches, among which one finds the so-called quasiharmonic approximation (QHA) [4, 5], perturbation expansions [6, 7] and self-consistent phonon theories [8–11]. In particular, isotopic effects in the lattice parameter of neon and argon were estimated by comparing results obtained from Lennard-Jones potentials with different parameters [6]. In recent years, the QHA has been employed to study isotopic effects in the crystal volume of covalent solids from *ab initio* density-functional-theory calculations [12–14].

A different theoretical approach to studying anharmonic effects in solids is the Feynman path integral (PI) method [15, 16], which turns out to be a well-suited method for studying this kind of effect at temperatures at which the quantum character of the atomic nuclei is relevant ($T \lesssim \Theta_D$). The combination of PIs with Monte Carlo (MC) sampling enables us to carry out quantitative and nonperturbative studies of such anharmonic effects. The PI MC method had been used earlier to study several structural and thermodynamic properties of rare-gas solids [17–22]. In the context of the PI formalism, several authors developed effective (temperature-dependent) classical potentials that reproduce accurately several properties of quantum solids [23–25]. More recently, Acocella *et al* [26] have applied an improved effective-potential MC theory [27] to study thermal and elastic properties of noble-gas solids. In our present context, the PI MC method has been employed to study the isotopic shift in the helium melting pressure [28, 29], as well as isotope effects in the structural properties of solid neon [18] and diamond-type materials [30, 31]. The isotopic-mass dependence of the lattice constant, in particular, can be described well from these kinds of simulations, which have yielded results [32, 33] in good agreement with experimental data [3, 34].

In this paper, we study the isotopic effect on the lattice parameter of noble-gas solids by means of PI MC simulations in the isothermal–isobaric ensemble. We analyse the dependence of this isotopic effect on temperature and pressure. The interatomic interaction is described by a Lennard-Jones potential. In a previous paper [33], we have studied with the same method several structural and thermodynamic properties of solid neon. Thus, most of the results presented here for the lattice parameter will refer to argon, krypton and xenon, and some data on neon will be given for the sake of comparison.

Table 1. Parameters σ and ϵ of the Lennard-Jones potential employed in this paper, average isotopic mass $\langle M \rangle$ and de Boer parameter Λ. Calculated zero-temperature properties of rare-gas solids at ambient pressure are also given: classical (a_0) and quantum ($a_{\rm nat}$) lattice parameters, along with kinetic energy per atom $E_k(0)$ obtained from PI MC simulations of solids with average isotopic mass.

Element	σ (Å)	ϵ (meV)	$\langle M \rangle$ (amu)	Λ	a_0 (Å)	$a_{\rm nat}(0)$ (Å)	$E_k(0)$ (meV)
Ne	2.782	3.084	20.18	0.585	4.2890	4.4631	3.50
Ar	3.404	10.32	39.95	0.186	5.2480	5.3115	4.13
Kr	3.638	14.17	83.80	0.103	5.6088	5.6458	3.19
Xe	3.961	19.91	131.30	0.063	6.1068	6.1316	2.80

2. Method

Finite-temperature properties of rare-gas solids with different isotopic masses have been calculated by PI MC simulations in the isothermal–isobaric (NPT) ensemble. Quantum exchange effects were not considered, since they are negligible at the densities considered here. In the PI formulation of statistical mechanics, the partition function of a quantum system is approximated by a discretization of the density matrix along cyclic paths. These quantum paths consist of a finite number L (Trotter number) of 'imaginary-time' steps [15], which gives rise to the appearance of L 'replicas' for each quantum particle in the numerical simulations. Thus, the practical implementation of this method is based on an isomorphism between the quantum system and a classical one, obtained by replacing each quantum particle (atomic nucleus in the present case) by a cyclic chain of L classical particles, connected by harmonic springs with a temperature-dependent constant [35]. Details on this computational method can be found elsewhere [36–38].

Simulations have been performed on $5 \times 5 \times 5$ cubic supercells of the face-centred-cubic unit cell, including $N = 500$ rare-gas atoms. Periodic boundary conditions were assumed. We have checked that this size is enough to have a negligible finite-size effect on the lattice parameters obtained in the simulations. In particular, this size effect is smaller than the statistical noise of the data presented below.

Rare-gas atoms were treated as quantum particles interacting through a Lennard-Jones potential:

$$V(r) = 4\epsilon\left[\left(\frac{\sigma}{r}\right)^{12} - \left(\frac{\sigma}{r}\right)^{6}\right], \tag{1}$$

with parameters ϵ and σ given in table 1. The parameters for Ar, Kr and Xe were taken from [39] (σ was slightly changed in the case of Ar to improve the agreement with the experimental lattice parameter of the solid with natural isotopic composition). The parameters for Ne are those employed previously to study solid Ne [33]: ϵ coincides with that used in earlier PI MC simulations [18, 40] and σ is slightly smaller than in [5, 17, 39].

The dynamic effect of interactions between nearest neighbours has been explicitly considered, and the effect of interactions beyond nearest neighbours has been taken into account by a static-lattice approximation [17, 18]. This assumption was employed earlier in PI MC simulations of Lennard-Jones solids, yielding the same results as those obtained in simulations including dynamical correlations up to several neighbouring atom shells [19]. Our simulations were based on the so-called 'primitive' form of PI MC and the 'crude' energy estimator was used [35, 41]. As in standard PI MC, quantum paths were discretized into L (Trotter number) points. To keep a constant precision for the results at different temperatures, we have considered a Trotter number that scales as the inverse temperature. At a given temperature, the actual

value of L required to obtain convergence of the results depends on the Debye temperature of the considered solid (higher Θ_D needs larger L). We have taken $LT = 250$ K for solid Ar and $LT = 200$ K for the other noble-gas solids, which were found to be sufficient to reach convergence. The larger Trotter number necessary in the case of solid Ar is due to the higher Debye temperature of this solid ($\Theta_D \sim 90$ K for Ar versus ~70 K for the other rare-gas solids). This means that $L = \hbar\omega_c/(k_B T)$, with $\omega_c \sim 3\omega_D$ (ω_D the Debye frequency of the material). Thus, for example, a PI MC simulation on a $5 \times 5 \times 5$ supercell of solid Ar at 5 K ($L = 50$) is equivalent in computational effort to a classical MC simulation of $LN = 25\,000$ atoms. Results for the lattice parameter obtained from simulations with larger Trotter numbers lie within the error bars of the data shown below. The convergence of the lattice parameter with L in PI MC simulations has been studied with more detail in previous work [42].

Sampling of the configuration space has been carried out by the Metropolis method [43] at temperatures between 3 K and the melting temperature of the different solids, as well as at pressures between 1 atm and 30 kbar. For given temperature, pressure and isotopic mass, a typical run consisted of the generation of 2×10^4 paths per atom for system equilibration, followed by 3×10^5 paths per atom for the calculation of ensemble average properties. More details on the application of this method were given elsewhere [36].

Rare-gas crystals with a natural isotopic composition have been modelled by setting the average mass $\langle M \rangle$ for every atom in the simulation cell. ($\langle M \rangle$ is given in table 1 for the different rare gases studied here.) This is the so-called 'virtual-crystal approximation', whose validity to describe phonon-related properties has been discussed by Cardona [1]. In particular, if the mass fluctuation is not too large, the phonon frequencies scale as $\omega \propto \langle M \rangle^{-1/2}$. We have checked that the results obtained for the lattice parameter by using this approximation coincide (within the precision of our results) with those yielded by distributing randomly atoms with different masses in an adequate proportion over the simulation cell.

3. Results and discussion

3.1. Average isotopic mass

In figure 1 we present the temperature dependence of the equilibrium lattice parameter a for rare-gas solids with natural isotopic composition, as obtained from PI MC simulations at atmospheric pressure: (a) Ar, (b) Kr, (c) Xe. Open squares represent results of our simulations and full curves indicate data derived from x-ray diffraction experiments by different authors [44–46]. Both sets of data closely follow each other. For comparison with the results of the quantum simulations, we have also displayed in figure 1 the temperature dependence of a in the classical limit (infinite-mass limit), with the same Lennard-Jones potentials (triangles and dotted curves). These classical MC simulations give at low temperatures a nearly linear temperature dependence for the interatomic distance (or lattice parameter), which converges for $T \to 0$ to the value corresponding to the minimum potential energy of each crystal (point atoms on their lattice sites).

The combined effects of anharmonicity in the interatomic potential and the quantum character of the atomic nuclei show up clearly in the low-temperature lattice parameter of the studied crystals, which is larger than that corresponding to the minimum potential energy of the (classical) crystal, a_0. The zero-temperature lattice parameters derived from classical a_0 and quantum $a_{\rm nat}(0)$ simulations at ambient pressure are given in table 1. For Ar we find at $T = 0$ an appreciable lattice expansion of 0.0635 Å. This means an increase of 1.2% in the lattice parameter due to anharmonicity of the zero-point atomic motion, which amounts to about one-third of the change in a originated from thermal expansion between $T = 0$ K and

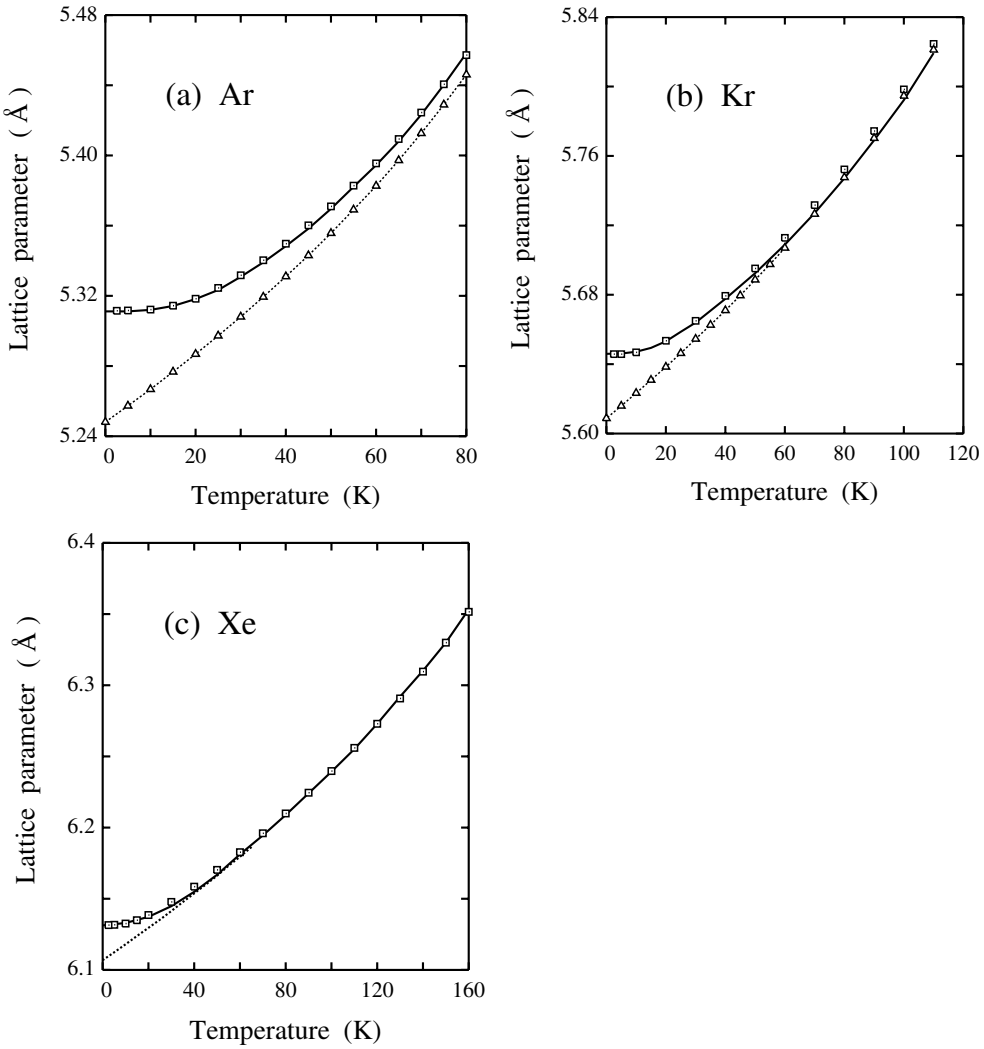

Figure 1. Temperature dependence of the lattice parameter of rare-gas crystals with natural isotopic composition: (a) Ar, (b) Kr, (c) Xe. Open squares indicate results of PI MC simulations with Lennard-Jones potentials. Triangles and dotted curves represent results derived from classical MC simulations with the same interatomic potentials. Error bars are less than the symbol size. Full curves represent results derived from x-ray diffraction experiments for Ar [44], Kr [45] and Xe [46].

the melting temperature of argon (84 K). This quantum effect decreases as the atomic mass rises, but even for Xe it is not negligible and we obtain $a_{\rm nat}(0) - a_0 = 0.0248$ Å. Thus, we find that the relative increase in lattice parameter at $T = 0$, $\psi = [a_{\rm nat}(0) - a_0]/a_0$, decreases from 4.06×10^{-2} for Ne to 4.06×10^{-3} for Xe.

For Lennard-Jones solids, the magnitude of quantum effects can be quantified by the so-called de Boer parameter, defined as $\Lambda = h/\sigma\sqrt{M\epsilon}$ [47–49]. This parameter ranges from 0.06 for Xe to 0.59 for Ne (see table 1). For comparison, we mention that $\Lambda = 2.67$ for ^{4}He, which shows well-known pronounced quantum effects. In figure 2 we have plotted the relative zero-temperature lattice expansion ψ versus the de Boer parameter Λ. As expected, ψ increases with Λ, and we find a nearly linear relation between both quantities. For each noble gas studied

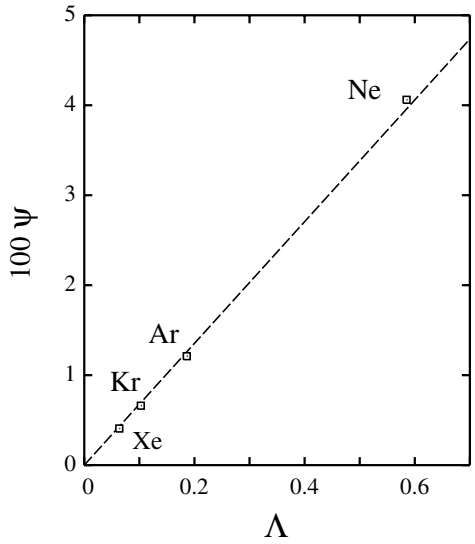

Figure 2. Low-temperature relative change in the lattice parameter, $\psi = [a_{\rm nat}(0) - a_0]/a_0$, versus the de Boer parameter Λ for rare-gas solids with natural isotopic composition. Symbols represent results derived from PI MC simulations.

here, the mass difference between the heaviest and lightest stable isotope is close to 10% of the average mass. This means that relative changes in Λ for a given element are about 5%, since this parameter scales as $M^{-1/2}$.

For given volume and temperature, the internal energy of a solid, $E(V, T)$, can be written as

$$E(V, T) = E_0 + E_{\rm el}(V) + E_{\rm vib}(V, T), \tag{2}$$

where E_0 is the minimum potential energy for the (classical) crystal at $T = 0$, $E_{\rm el}(V)$ is the elastic energy and $E_{\rm vib}(V, T)$ is the vibrational energy. The elastic energy depends only on the volume (and implicitly on T because of the temperature dependence of V) and at low T is basically due to the change in volume originating from zero-point vibration [33]. The vibrational energy depends explicitly on both V and T and can be obtained by subtracting the elastic energy from the internal energy. PI MC simulations allow one to obtain separately the vibrational kinetic, E_k, and potential energy, E_p, as explained in detail elsewhere [36, 37, 50]. Our results for the kinetic energy of noble-gas solids at $T = 0$ are given in table 1. They are close to those obtained by Nosanow and Shaw [51] from Hartree calculations with a Lennard-Jones potential. In fact, differences between both methods are less than 2% for the solids studied here, except for Ne, for which they differ by about 5%. Our results for the zero-temperature kinetic energy of rare-gas solids, as well as those found in earlier work (see e.g. [51]) do not show a smooth trend for the different elements as the atomic mass changes. Thus, one finds the maximum $E_k(0)$ for Ar. This can be qualitatively understood by looking at the Debye temperature of these solids, which also present a maximum value for argon. In fact, Θ_D is close to 70 K for Ne, Kr and Xe, whereas $\Theta_D \approx 90$ K for solid argon. In a simple Debye model, assuming a vibrational density of states $\rho(\omega) \propto \omega^2$, and a cutoff ω_D, one has a linear relation between $E_k(0)$ and ω_D (in fact, one finds $E_k^D(0) = \frac{9}{16}\hbar\omega_D$ [33, 52]) and one expects the highest $E_k(0)$ for solid argon. For the other elements, one observes a decrease in $E_k(0)$ as mass rises. This decrease is found to be larger than expected from the crude Debye model.

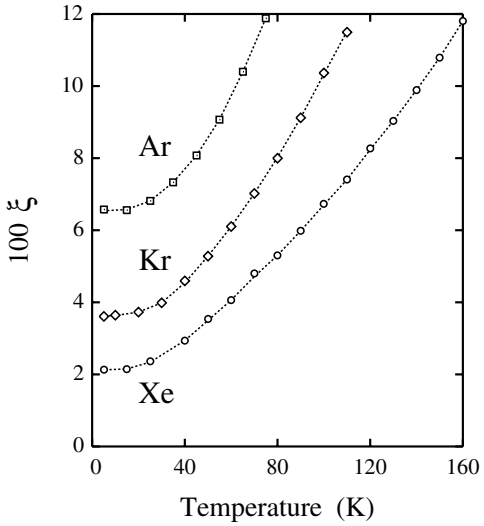

Figure 3. Anharmonicity parameter ξ for rare-gas crystals with natural isotopic composition. Squares: Ar; diamonds: Kr; circles: Xe. Error bars are less than the symbol size. Dotted curves are guides to the eye.

A quantitative evaluation of the overall anharmonicity of the atom vibrations can be obtained by comparing the potential and kinetic energy at different temperatures. With this purpose we consider the anharmonicity parameter [18]: $\xi = 2(E_k - E_p)/(E_k + E_p)$, which should be zero for a harmonic solid at any temperature, as follows from the virial theorem. In figure 3 we present the temperature dependence of the parameter ξ for Ar (squares), Kr (diamonds) and Xe (circles), as derived from our PI MC simulations. This parameter is positive in all cases, and increases as the atomic mass is lowered. ξ also increases as the temperature rises, as expected for an increase in anharmonicity at finite temperatures, when compared with the low-T limit. For $T \to 0$ we find $\xi = 0.066$, 0.036 and 0.021, for Ar, Kr and Xe, respectively. For these three solids, we find at the corresponding melting temperature $\xi \approx 0.12$. The same kind of MC simulations give for Ne at $T \to 0$ a parameter $\xi = 0.21$ [33], corresponding to a much larger anharmonicity of the atom vibrations. Note that this is a pure quantum effect due to zero-point motion, since at $T = 0$ the atoms feel the anharmonicity of the interatomic potential, in contrast with any classical model, where $\xi \to 0$ for $T \to 0$, irrespective of anharmonicity.

Anharmonic effects in solid Ar have been quantified earlier by comparing the kinetic and potential energies derived from PI MC simulations [18]. For $T \to 0$ these authors found an anharmonicity parameter $\xi = 0.0675$, close to the value obtained here. These anharmonicities are large as compared with those found for covalent solids at low temperatures ($T \ll \Theta_D$). For example, for diamond, silicon and germanium one finds at low T differences between E_p and E_k smaller than 1%, and at the Debye temperature of each material, they are less than 3% [30, 31, 42]. It is worthwhile mentioning also that for such covalent materials the vibrational potential energy E_p is larger than E_k (i.e. $\xi < 0$), opposite to the present case of rare-gas solids where $\xi > 0$. This means that the result $E_p < E_k$ found here is not general in solids, and can be associated with the particular character of the interatomic interactions present in rare-gas (Lennard-Jones) solids.

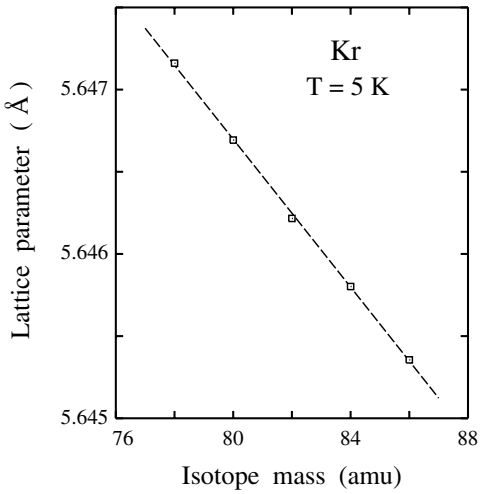

Figure 4. Lattice parameter of Kr crystals as a function of isotopic mass at $T = 5$ K and $P = 1$ atm. Symbols indicate results of PI MC simulations. The broken line is a least-square fit to the simulation results. Error bars are less than the symbol size.

3.2. Isotopic effect at low temperature

In figure 4 we show the dependence of the lattice parameter on isotopic mass for Kr crystals at 5 K. From the PI MC results (symbols), we find a linear dependence of a on the mass M. Similar linear dependencies are found for the other rare-gas crystals and are presented in figure 5. In this figure we display the difference $\delta a = a - a_{\rm nat}$ as a function of the ratio $M/\langle M\rangle$. Different symbols correspond to different elements: squares for Ar, diamonds for Kr, circles for Xe, and broken lines are least-square fits to the data points. The slope of these lines becomes more negative as the atomic mass is lowered.

The low-temperature changes in a due to isotopic mass can be related to the zero-point lattice expansion of a crystal with average isotopic mass $\langle M\rangle$. In fact, in a QHA the lattice parameter $a_{\rm nat}(0)$ at $T = 0$ can be expressed as [14, 31]

$$a_{\rm nat}(0) = a_0 + \frac{\chi(0)}{6a_0^2}\sum_{n,\boldsymbol{q}}\hbar\omega_n(\boldsymbol{q})\gamma_n(\boldsymbol{q}). \tag{3}$$

Here, $\omega_n(\boldsymbol{q})$ are the frequencies of the nth mode in the crystal, $\chi(0)$ is the zero-temperature compressibility and $\gamma_n(\boldsymbol{q}) = -\partial \ln \omega_n(\boldsymbol{q})/\partial \ln V$ is the Grüneisen parameter of mode n, $\boldsymbol{q}$.

From a first-order expansion for the lattice parameter as a function of isotopic mass, and assuming that the frequencies $\omega_n(\boldsymbol{q})$ scale with isotopic mass as $1/\sqrt{M}$, one finds for the relative change in lattice parameter with isotopic mass at $T = 0$:

$$\frac{\delta a}{\delta M} = -\frac{a_{\rm nat}(0) - a_0}{2\langle M\rangle}, \tag{4}$$

where $\delta M = M - \langle M\rangle$. This means that the low-temperature changes in a due to isotopic mass can be explained quantitatively from the change in lattice parameter caused by the atomic zero-point motion in the natural crystal, as compared to the 'classical' crystal, in which a is given by the minimum of the potential energy. By taking $a_{\rm nat}(0) - a_0 = 0.037$ Å for Kr (see above), equation (4) gives $\delta a/\delta M = -2.21\times10^{-4}$ Å amu^{-1}, close to a value of -2.25×10^{-4} Å amu^{-1} obtained from the PI MC simulations of Kr crystals with different isotopic masses (see figure 4).

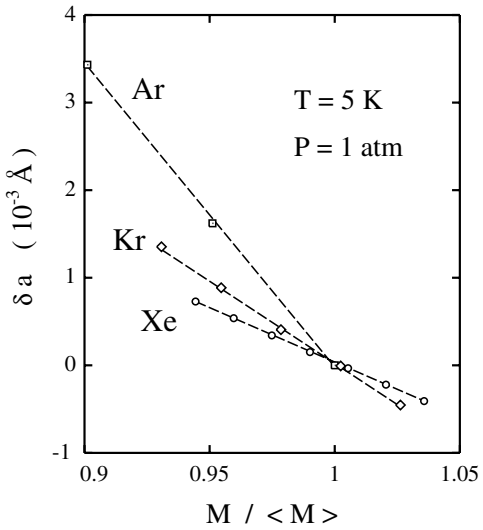

Figure 5. Difference in lattice parameter $\delta a = a - a_{\rm nat}$ as a function of the mass ratio $M/\langle M\rangle$, at $T = 5$ K and $P = 1$ atm. Symbols represent results of PI MC simulations for Ar (squares), Kr (diamonds) and Xe (circles). Broken lines are least-square fits to the simulation results.

Using the same procedure, equation (4) gives for Ar and Xe the ratios $\delta a/\delta M = -7.95 \times 10^{-4}$ and -9.44×10^{-5} Å amu^{-1}, respectively. This ratio for Xe coincides (within error bars) with that derived from the PI MC simulations, whereas the ratios $\delta a/\delta M$ obtained for solid Ar with both procedures differ by 9%. This is caused by the higher anharmonicity present in the latter case, which means that the assumptions employed to derive equation (4) are less precise:

(1) neglect of higher-order terms in the expansion of the lattice parameter as a function of isotopic mass, and
(2) the assumption that $\omega_n(\boldsymbol{q})$ scales with mass as in a harmonic solid ($\sim 1/\sqrt{M}$).

In any case, if the zero-point expansion for a natural crystal is known, equation (4) provides one with a good estimate of the isotopic effect.

To summarize, we find an appreciable zero-temperature isotopic effect in the rare-gas solids studied here. This isotope effect is due to the anharmonicity of the zero-point vibrations, which is well captured by a QHA in which the phonon frequencies depend on both mass and crystal volume. The dependence of the compressibility and Grüneisen parameters upon isotope mass does not appear to be relevant in this context.

3.3. Temperature dependence of the isotopic effect

In figure 6 we show the difference Δa between the lattice parameters of isotopically pure crystals with the lightest and heaviest stable isotopes, for argon (^{36}Ar and ^{40}Ar), krypton (^{78}Kr and ^{86}Kr) and xenon (^{124}Xe and ^{136}Xe). In each case, Δa decreases as the temperature is raised, since quantum effects become less relevant to describe the atomic motion. One still observes this isotope effect in the lattice parameter at temperatures on the order of the Debye temperature of the considered crystals. This happens even for Xe, in spite of the large atomic mass of this element. Note that today's state-of-the-art experimental techniques allow one to measure lattice-parameter differences smaller than those found here. In fact, the difference

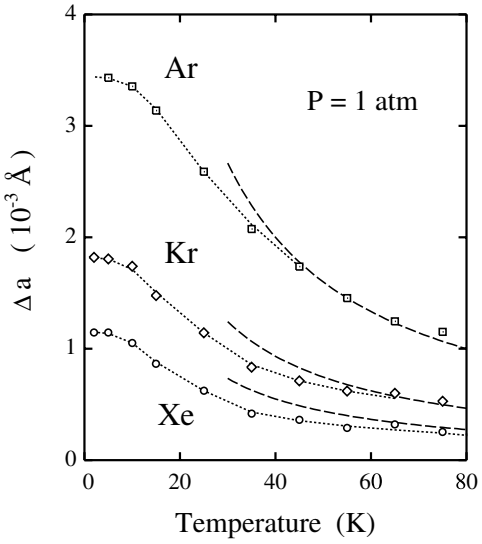

Figure 6. Temperature dependence of the difference between lattice parameters of isotopically pure crystals composed of the lightest and heaviest stable isotopes. Argon (squares): ^{36}Ar and ^{40}Ar; krypton (diamonds): ^{78}Kr and ^{86}Kr; xenon (circles): ^{124}Xe and ^{136}Xe. Error bars are less than (on the order of) the symbol size at $T < 40$ K ($T > 40$ K). Dotted curves are guides to the eye. Broken curves correspond to a high-temperature approximation and were derived from equation (9) as indicated in the text.

$\Delta a = 2.5 \times 10^{-4}$ Å obtained for Xe at 75 K is larger than those found experimentally for silicon and germanium crystals with controlled isotope concentrations [2, 3]. Note that we call δa changes in the lattice parameter with respect to the crystal with natural isotopic composition, and Δa differences between lattice parameters of crystals composed of the lightest and heaviest stable isotopes of each element.

To analyse the results of our MC simulations we consider again a QHA for the lattice vibrations. In this approach, the lattice parameter at temperature T, $a(T)$, for isotopic mass M and zero pressure can be written as [14]

$$a(T) = a_0 + \frac{\chi}{3a_0^2} \sum_{n,\boldsymbol{q}} \gamma_n(\boldsymbol{q}) E_n(\boldsymbol{q}, T), \tag{5}$$

where

$$E_n(\boldsymbol{q}, T) = \frac{1}{2}\hbar\omega_n(\boldsymbol{q}) \coth\left(\frac{\hbar\omega_n(\boldsymbol{q})}{2k_B T}\right). \tag{6}$$

At high temperatures ($T \gtrsim \Theta_D$), one can expand $E_n(\boldsymbol{q}, T)$ in powers of $1/k_B T$ to obtain

$$a(T) \approx a_0 + \frac{\chi}{3a_0^2} \sum_{n,\boldsymbol{q}} \gamma_n(\boldsymbol{q}) \left[k_B T + \frac{[\hbar\omega_n(\boldsymbol{q})]^2}{12 k_B T} \right], \tag{7}$$

and assuming a mass dependence of the frequencies $\omega_n(\boldsymbol{q}) \sim 1/\sqrt{M}$, we find for the change of lattice parameter with isotopic mass:

$$\frac{\delta a}{\delta M} \approx -\frac{\chi}{36 a_0^2 \langle M \rangle k_B T} \sum_{n,\boldsymbol{q}} \gamma_n(\boldsymbol{q}) \left[\hbar\omega_n(\boldsymbol{q})\right]^2. \tag{8}$$

Thus for T up to the melting temperature of each solid, $\delta a/\delta M$ is expected to decrease as $1/T$.

The high-temperature ratio $\delta a/\delta M$ given in equation (8) can be estimated by assuming a Debye density of states (proportional to ω^2) and an average mode-independent Grüneisen constant γ [49]. Taking into account that the face-centred-cubic unit cell includes four atoms (and therefore 12 independent modes per cell), one finds

$$\frac{\delta a}{\delta M} \approx -\frac{\gamma \chi (\hbar\omega_D)^2}{5a_0^2\langle M\rangle k_B T}. \tag{9}$$

Taking $\omega_D = 63$, 50 and 44 cm^{-1} and $\gamma = 2.6$, 2.8 and 2.9 for Ar, Kr and Xe, respectively [44, 45, 53], we find from equation (9) the temperature dependence of Δa displayed in figure 6 by broken curves. At $T > 50$ K these curves lie close to the data points derived from PI MC simulations. This means that the isotopic effect on the lattice parameter at temperatures on the order of Θ_D can be estimated rather accurately by employing equation (9), which makes use only of known parameters of the crystal under consideration.

3.4. Pressure dependence of the isotopic effect

To check the reliability of the Lennard-Jones potential employed here to reproduce the properties of rare-gas solids under (low) pressure, we have calculated the isothermal compressibility χ at ambient pressure. This quantity can be derived in MC simulations in the isothermal–isobaric ensemble from fluctuations in the lattice parameter. The mean-square fluctuations in the volume V of the simulation cell are given in this ensemble by

$$\sigma_V^2 = \chi V k_B T, \tag{10}$$

and therefore

$$\chi = \frac{9l^3 a}{k_B T}\sigma_a^2. \tag{11}$$

Here l is the side length of the simulation cell in units of the lattice parameter ($l = 5$ in our case), and σ_a^2 indicates the mean-square fluctuations in the lattice parameter at temperature T.

Results for the isothermal compressibility of rare-gas solids derived in this way are presented in figure 7 (symbols) as a function of temperature, along with experimental data for crystals with natural isotopic composition (curves) [44, 46, 54]. The overall agreement between calculated values and experimental results is satisfactory, given the uncertainty in the data actually measured (error bars are shown for some experimental points, and those of the calculated compressibility are less than the symbol size). In the zero-temperature limit we find $\chi = 3.78$, 3.09 and 2.75×10^{-11} cm^2 dyne^{-1} for Ar, Kr and Xe, respectively, with an estimated error bar of $\pm 2 \times 10^{-13}$ cm^2 dyne^{-1}. For solid neon, the same procedure yields $\chi = 1.01 \times 10^{-10}$ cm^2 dyne^{-1} [33], a value much larger than for the other noble-gas solids. Note that the classical expectancy at $T = 0$ is given by $\chi_{\rm cl}(0) = \sigma^3/75\epsilon$ (see, e.g., [49]). Values of $\chi_{\rm cl}(0)$ derived by using the σ and ϵ values given in table 1 are appreciably lower than those found in PI MC simulations, even for Xe. This means that quantum effects give rise to an important increase in the low-temperature compressibility (19% for Ar, 9% for Kr, and 5% for Xe).

In figure 8 we present the difference Δa between the lattice parameter of isotopically pure crystals of noble gases as a function of pressure. In this figure, data for Ne are also included, as they have not been presented in earlier publications. In each case, Δa decreases as pressure rises, and the relative decrease in this isotopic effect is more pronounced for Ne than for the other elements. Thus for solid Ne, Δa decreases from 8.73×10^{-3} Å at $P = 1$ atm to 1.35×10^{-3} Å at $P = 30$ kbar. This means a reduction of Δa by a factor of 6.5 in this pressure range. At the other extreme, for Xe one finds a decrease in Δa by a factor of 3.1 in the same pressure region. This is indeed due to the larger compressibility of Ne, as compared with Xe. In

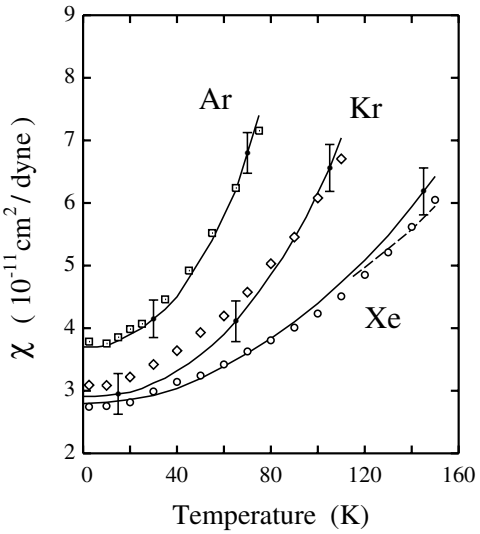

Figure 7. Isothermal compressibility χ at ambient pressure as a function of temperature. Symbols indicate results derived from PI MC simulations for rare-gas solids with natural isotopic composition: squares, Ar; diamonds, Kr; circles, Xe. Error bars of the calculated compressibilities are smaller than the symbol size. Curves represent experimental data obtained by different authors: Ar [44], Kr [45]. For Xe, the full curve is from [46], whereas the broken curve represents more recent results from [54]. Error bars are given for some experimental points, indicated by black dots.

fact, as shown in figure 7, χ decreases as the atomic mass of the noble gas rises. This decrease in the isotopic effect is mainly caused by a reduction of the compressibility as pressure is raised. At low temperatures, this can be qualitatively understood from equations (3) and (4). From these equations one sees that the change in δa with applied pressure can be derived from the changes in the compressibility χ, the 'classical' lattice parameter a_0 (both decreasing with pressure) and the phonon frequencies $\omega_n(\boldsymbol{q})$ (which usually increase with pressure). The pressure-induced changes in χ clearly dominate those of a_0^2 and $\omega_n(\boldsymbol{q})$ in equation (3), giving rise to the important decrease in δa presented in figure 8 for noble-gas solids.

Using diamond-anvil cell methods, one can nowadays study materials under very high pressures. In fact, rare-gas solids have been studied in recent years at hydrostatic pressures of hundreds of kilobars [55–58]. At such high pressures, the isotopic effects on structural and thermodynamic properties of these solids will be drastically reduced with respect to ambient-pressure values. The reliability of the present Lennard-Jones potential to study rare-gas solids at high pressures is, however, not guaranteed, since three-body terms in the interatomic potential can be necessary to reproduce the structural and thermodynamic properties of these solids.

4. Conclusions

PI MC simulations provide us with a powerful tool to study isotopic effects in rare-gas solids, originating from the anharmonicity of the interatomic potential. This method allows us to study phonon-related properties, without the assumption of harmonic or QHAs, usually employed in theoretical studies. In this way, one can separate the kinetic and potential contributions to the vibrational energy of the solid and quantify the anharmonicity of the lattice vibrations, which together with zero-point motion give rise to isotopic effects on structural and thermodynamic properties of solids.

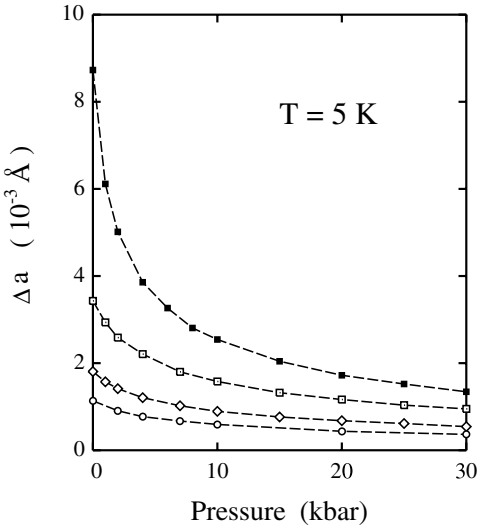

Figure 8. Pressure dependence of the difference between lattice parameters of isotopically pure crystals composed of the lightest and heaviest stable isotopes. Symbols represent results derived from PI MC simulations at 5 K. Neon (black squares): ^{20}Ne and ^{22}Ne; argon (open squares): ^{36}Ar and ^{40}Ar; krypton (diamonds): ^{78}Kr and ^{86}Kr; xenon (circles):^{124}Xe and ^{136}Xe. Error bars are less than the symbol size. Curves are guides to the eye.

Owing to the large anharmonicity of the lattice vibrations in noble-gas solids, the isotopic effect on the lattice parameter of these solids is appreciable. We emphasize that even for solid xenon it is measurable at temperatures on the order of its Debye temperature ($\Theta_D \approx 64$ K) with current experimental techniques. At low temperatures, the dependence of the lattice parameter on isotopic mass is related to the zero-point lattice expansion, as indicated by equation (4). The magnitude of this isotopic effect changes drastically as temperature or pressure increase. At 80 K it is clearly reduced with respect to the zero-temperature limit. At this temperature Δa for Ar, Kr and Xe is less than one-third of the corresponding low-temperature value. An applied pressure also causes an important decrease in Δa. Thus, a modest pressure of 30 kbar reduces this difference by a factor 6.5 for Ne and 3.1 for Xe.

We finally note that the isotopic effect studied here for rare-gas solids turns out to be larger than that found in covalent materials, as a consequence of the larger anharmonicity of the interatomic interactions in the present case. Other structural and thermodynamic properties of these solids are expected to show isotopic effects that, although smaller than in the case of neon, can be measurable for the other noble gases.

Acknowledgments

The author benefited from discussions with R Ramírez and L M Sesé. This work was supported by CICYT (Spain) through Grant No BFM2000-1318.

References

[1] Cardona M 2000 *Phys. Status Solidi* b **220** 5
[2] Kazimirov A, Zegenhagen J and Cardona M 1998 *Science* **282** 930
[3] Sozontov E, Cao L X, Kazimirov A, Kohn V, Konuma M, Cardona M and Zegenhagen J 2001 *Phys. Rev. Lett.* **86** 5329
[4] Srivastava G P 1990 *The Physics of Phonons* (Bristol: Hilger)

[5] Della Valle R G and Venuti E 1998 *Phys. Rev.* B **58** 206
[6] Brown J S and Feldman J L 1966 *Proc. Phys. Soc.* **89** 993
[7] Klein M L, Horton G K and Feldman F L 1969 *Phys. Rev.* **184** 968
[8] Goldman V V, Horton G K and Klein M L 1968 *Phys. Rev. Lett.* **21** 1527
[9] Goldman V V, Horton G K and Klein M L 1969 *J. Low Temp. Phys.* **1** 391
[10] Klein M L, Koehler T R and Gray R L 1973 *Phys. Rev.* B **7** 1571
[11] Paskin A, Llois de Kreiner A M, Shukla K, Welch D O and Dienes G J 1982 *Phys. Rev.* B **25** 1297
[12] Pavone P and Baroni S 1994 *Solid State Commun.* **90** 295
[13] Biernacki S and Scheffler M 1994 *J. Phys.: Condens. Matter* **6** 4879
[14] Debernardi A and Cardona M 1996 *Phys. Rev.* B **54** 11305
[15] Feynman R P 1972 *Statistical Mechanics* (New York: Addison-Wesley)
[16] Kleinert H 1990 *Path Integrals in Quantum Mechanics, Statistics and Polymer Physics* (Singapore: World Scientific)
[17] Cuccoli A, Macchi A, Pedrolli G, Tognetti V and Vaia R 1997 *Phys. Rev.* B **56** 51
[18] Müser M H, Nielaba P and Binder K 1995 *Phys. Rev.* B **51** 2723
[19] Neumann M and Zoppi M 2000 *Phys. Rev.* B **62** 41
[20] Chakravarty C 2002 *J. Chem. Phys.* **116** 8938
[21] Timms D N, Evans A C, Boninsegni M, Ceperley D M, Mayers J and Simmons R O 1996 *J. Phys.: Condens. Matter* **8** 6665
[22] Neumann M and Zoppi M 2002 *Phys. Rev.* E **65** 031203
[23] Giachetti R and Tognetti V 1986 *Phys. Rev.* B **33** 7647
[24] Feynman R P and Kleinert H 1986 *Phys. Rev.* A **34** 5080
[25] Cuccoli A, Macchi A, Neumann M, Tognetti V and Vaia R 1992 *Phys. Rev.* B **45** 2088
[26] Acocella D, Horton G K and Cowley E R 2000 *Phys. Rev.* B **61** 8753
[27] Acocella D, Horton G K and Cowley E R 1995 *Phys. Rev. Lett.* **74** 4887
[28] Barrat J L, Loubeyre P and Klein M L 1989 *J. Chem. Phys.* **90** 5644
[29] Boninsegni M, Pierleoni C and Ceperley D M 1994 *Phys. Rev. Lett.* **72** 1854
[30] Noya J C, Herrero C P and Ramírez R 1997 *Phys. Rev.* B **56** 237
[31] Herrero C P 2000 *Phys. Status Solidi* b **220** 857
[32] Herrero C P 1999 *Solid State Commun.* **110** 243
[33] Herrero C P 2002 *Phys. Rev.* B **65** 014112
[34] Batchelder D N, Losee D L and Simmons R O 1968 *Phys. Rev.* **173** 873
[35] Chandler D and Wolynes P G 1981 *J. Chem. Phys.* **74** 4078
[36] Noya J C, Herrero C P and Ramírez R 1996 *Phys. Rev.* B **53** 9869
[37] Gillan M J 1988 *Phil. Mag.* A **58** 257
[38] Ceperley D M 1995 *Rev. Mod. Phys.* **67** 279
Ceperley D M 1999 *Rev. Mod. Phys.* **71** S438
[39] Cuccoli A, Macchi A, Tognetti V and Vaia R 1993 *Phys. Rev.* B **47** 14923
[40] Thirumalai D, Hall R W and Berne B J 1984 *J. Chem. Phys.* **81** 2523
[41] Singer K and Smith W 1988 *Mol. Phys.* **64** 1215
[42] Herrero C P and Ramírez R 2001 *Phys. Rev.* B **63** 024103
[43] Binder K and Heermann D W 1988 *Monte Carlo Simulation in Statistical Physics* (Berlin: Springer)
[44] Peterson O G, Batchelder D N and Simmons R O 1966 *Phys. Rev.* **150** 703
[45] Losee D L and Simmons R O 1968 *Phys. Rev.* **172** 944
[46] Pollack G L 1964 *Rev. Mod. Phys.* **36** 748
[47] de Boer J 1948 *Physica (Amsterdam)* **14** 139
[48] Toda M, Kubo R and Saitô N 1992 *Statistical Physics I: Equilibrium Statistical Mechanics* (Berlin: Springer)
[49] Ashcroft N W and Mermin N D 1976 *Solid State Physics* (Philadelphia, PA: Saunders)
[50] Herrero C P 2000 *J. Non-Cryst. Solids* **271** 18
[51] Nosanow L H and Shaw G L 1962 *Phys. Rev.* **128** 546
[52] Berheide M, Schulte W H, Becker H W, Borucki L, Buschmann M, Piel N, Rolfs C, Mitchell G E and Schweitzer J S 1998 *Phys. Rev.* B **58** 11103
[53] Asaumi K 1984 *Phys. Rev.* B **29** 7026
[54] Granfors P R, Macrander A T and Simmons R O 1981 *Phys. Rev.* B **24** 4753
[55] Shimizu H, Tashiro H, Kume T and Sasaki S 2001 *Phys. Rev. Lett.* **86** 4568
[56] Iitaka T and Ebisuzaki T 2002 *Phys. Rev.* B **65** 012103
[57] Dewhurst J K, Ahuja R, Li S and Johansson B 2002 *Phys. Rev. Lett.* **88** 075504
[58] Errandonea D, Schwager B, Boehler R and Ross M 2002 *Phys. Rev.* B **65** 214110